Prediction of orthotropic ribbed plates' vibro-acoustics mechanisms: application to the piano soundboard

Benjamin Trévisan, Kerem Ege and Bernard Laulagnet

Laboratoire Vibrations Acoustique, INSA-Lyon, 25 bis Avenue Jean Capelle,
F-69621 Villeurbanne Cedex, France

The aim of this study is to develop an analytical method for the prediction of vibro-acoustical behavior of orthotropic ribbed plates with undescribed edges and more particularly its application to piano soundboard. It relies on a variational approach and motion field is calculated by modal analysis. In this article, we propose a general view of the method and give first results on a simplified soundboard. Also, we present an analysis of ribbed plate's modes as well as vibratory responses at typical frequencies treated in the literature but also responses at musical excitations and the influence of geometrical complexities.

1 Introduction

For a long time designed in an empirical manner, musical instruments are now a current subject of research, complex to study due to perceptive and subjective aspects of the sound produced. Indeed, many parameters determine their vibratory behaviour and thus the sound of the instrument (timbre): among them the material (type of wood used [1]) and the mechanical characteristics of the structure. In the case of the piano soundboard, this problem has been studied many times by Suzuki, Conklin, Giordano [2, 3, 4] and more recently by Berthaut, Ege & Boutillon and Chaigne [5, 6, 7, 8]. Its broadband behaviour is complex and problematics related to piano are leaded by musical questions. Above all, the research of a good trade-off between "loudness (radiated power) and sustain (duration)" in the last-but-one octave (killer octave) or the question of the timber not enough rich for the treble notes are major issues for piano designers and makers. In order to answer these questions, we develop an analytical vibro-acoustical model based on a variational formulation taking into account the influence of superstructures (ribs and bridge). This model enables to quantify the influence of the smallest variations of geometry on the vibro-acoustical behaviour of the structure. Unlike finite element modelling, analytical approach allow parametric studies.

2 Geometrical considerations

The piano soundboard has an essential role in the working of the instrument. Indeed, strings' sections are too small to radiate by themselves. So their vibrations are transmitted to the soundboard through the bridges which radiate efficiently the sound.

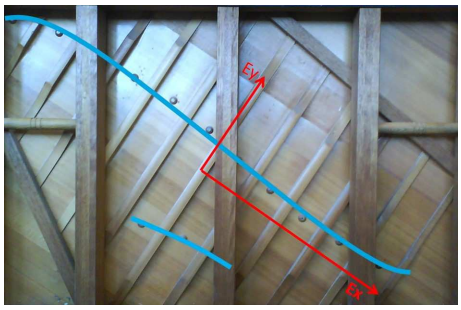

Figure 1: Soundboard of an upright piano.

Soundboards are constituted by a plate with complex geometry, traditionally made of spruce, pseudo-periodically ribbed on a face by several beams in a direction perpendicular to fibres of wood, and by one or two bridges on the opposite face in a direction nearly parallel to fibres (in blue in figure 1). Spruce is also used in the fabrication of ribs whereas bridges are made of beech or maple.

In this study, we will focus on an upright piano. The geometry of the soundboard is simplified: the plate is rectangular, orthotropy is "special" (principal axes are parallel to plate's edges), the ribs have the same length, there is only one straight bridge in the direction of fibres and the boundary conditions are simply supported (see figure 2).

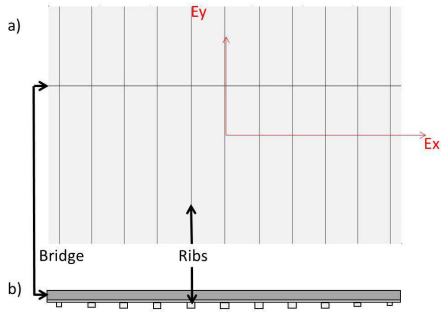

Figure 2: Simplified upright piano soundboard used in the analytical model. (a) : top view. ; (b) : sectional view of the soundboard and ribs.

Eccentricity of different superstructures is taken into account. Moreover, thickness of the plate, width and height of superstructures along the length are constant.

3 Theoretical formulation

The analytical model developed is based on a variational approach inspired by Laulagnet & Guyader's works [9, 10]. We have to calculate kinetic and strain energies of the whole structure.

3.1 Kinetic hypothesis of different substructures

Because the thickness of the board is very small compared to the other dimensions, we adopted the Love-Kirchhoff hypothesis linked to thin plates. Pumping effects and shearing in the two bending planes are ignored.
Under the hypothesis of linear variation of motions in the thickness (limited development at the order 1), it comes the following motion field:

$$\begin{cases} u(x,y,z,t) = -z\,\frac{\partial w}{\partial x} \\ v(x,y,z,t) = -z\,\frac{\partial w}{\partial y} \\ w(x,y,z,t) = w(x,y,t) \end{cases} \quad (1)$$

where $u(x,y,z,t)$ and $v(x,y,z,t)$ are the movements in directions $\vec{x}$ and $\vec{y}$ and $w(x,y,z,t)$ is the transversal displacement.

The different superstructures (ribs and bridge) are driven by bending and torsion. Conditions at the edges are applied to the plate and not to superstructures, so the plate controls the motion of those last. Displacements and rotations are considered as continuous at the interface so we write for a ribs in the direction $\vec{y}$ at the position $x = x_r$:

$$\begin{cases} u_{rft}(y,z,t) = -z\, w_{,x}(x_r,y,t) \\ v_{rft}(y,z,t) = -z\, w_{,y}(x_r,y,t) \\ w_{rft}(x,y,t) = w(x_r,y,t) + x\, w_{,x}(x_r,y,t) \end{cases} \tag{2}$$

where $x \in \left[x_r - \frac{b}{2}; x_r + \frac{b}{2}\right]$ and $z \in \left[\frac{h}{2}; \frac{h}{2} + H\right]$ and where h and H are respectively thickness of the plate and height of the ribs considered.

3.2 Hamilton function

From different motions' fields, we express Hamilton function of each sub-parts. This function is expressed by the integral of the difference between kinetic and strain energies on an arbitrary time interval. So, we write successively the actions of the plate, the bending and torsion of a rib in the direction $\vec{y}$ at the position $x = x_r$ by :

$$\begin{aligned} H_{plate} = \int_{t_0}^{t_1} \tfrac{1}{2} \int_S \rho h \dot{w}^2 - \Big(D_1 w_{,xx}^2 + D_3 w_{,yy}^2 \\ + D_2 w_{,xx} w_{,yy} + D_4 w_{,xy}^2\Big)\, dS\, dt \end{aligned} \tag{3}$$

$$\begin{aligned} H_{ribs\ bending} = \int_{t_0}^{t_1} \tfrac{1}{2} \int_S \Big[\rho_r \left(I_f \dot{w}_{,x}^2 + bH\dot{w}^2\right) \\ - E_r I_f w_{,yy}^2\Big] \delta(x - x_r)\, dS\, dt \end{aligned} \tag{4}$$

$$\begin{aligned} H_{ribs\ torsion} = \int_{t_0}^{t_1} \tfrac{1}{2} \int_S \Big[\rho_r I_g w_{,x}^2 \\ - G_r I_g w_{,xy}^2\Big] \delta(x - x_r)\, dS\, dt \end{aligned} \tag{5}$$

where the rib is considered as punctual in its width justifing the dirac $\delta(x - x_r)$.

We note that the rotational energy term is conserved in the bending function. Because of the small heights of ribs compared to their widths, torsional inertia doesn't take into account warping.
For a structure with an undetermined number of ribs in the direction $\vec{y}$ and a bridge in the direction $\vec{x}$, we express the entire function by :

$$H_{tot} = H_{plate} + \sum_{i=1}^{N} H_{i^{th}\ ribs} + H_{bridge} \tag{6}$$

3.3 Decomposition on the basis of simply supported unribbed plate modes

We decompose now those last equations on the basis of unribbed plate modes. We choose the simply supported basis because it's appropriated to an analytical approach currently used in the area of vibrations [9, 10]. The transversal displacement of the plate is written as a linear combination of unribbed plate modes weighted by modal amplitudes $a_{mn}(t)$:

$$w(x,y,t) = \sum_{m=1}^{M} \sum_{n=1}^{N} a_{mn}(t) \phi_{mn}(x,y) \tag{7}$$

where $\phi_{mn}(x,y) = sin\left(\frac{m\pi}{l}x\right) sin\left(\frac{n\pi}{L}y\right)$.

We note that mode shapes of the simply supported (unribbed) plate are orthogonal. By using of this solution in the Hamilton function, we calculate analytically the area integral.
In that case, the function depends on the couple of variables $(a_{mn}(t), \dot{a}_{mn}(t))$ and not on the transversal displacement $w(x,y,t)$ nor on its temporal and space derivatives $w_{,x}$, $w_{,xx}$, $w_{,yy}$, $w_{,xy}$ et $\dot{w}$. So, we note :

$$H_{tot} = \int_{t_0}^{t_1} \mathcal{L}(a_{mn}(t), \dot{a}_{mn}(t))\, dt \tag{8}$$

where $\mathcal{L}(a_{mn}(t), \dot{a}_{mn}(t))$ is called the Lagrangian of the system.

3.4 Lagrange's equations

In analytical mechanics every vibrating system is governed by the principle of less action also named Hamilton's principle. In practice, we use the differential form of Euler-Lagrange to determine the evolution of the system. Let, the following equations :

$$\delta H_{totale} = 0 \Leftrightarrow \frac{\partial \mathcal{L}}{\partial a_{pq}} - \frac{d}{dt} \frac{\partial \mathcal{L}}{\partial \dot{a}_{pq}} = 0 \tag{9}$$

expressed for each mode of the unribbed plate and where $p = 1 \rightarrow M$ and $q = 1 \rightarrow N$.

This minimization combined with the orthogonal properties of the simply supported plate modes permits to write a single equation for a particular mode "pq".
We finally get a homogeneous problem for which the size is conditioned by the number of unribbed plate's modes taken into account needed for the convergence of the solution. Let:

$$\begin{aligned} \left\{[M_p^{plate}] + [M_{pn}^{ribs} + [M_{pn}^{bridge}]\right\} \left\{\ddot{a}_p\right\} \\ + \left\{[K_p^{plate}] + [K_{pn}^{ribs} + [K_{pn}^{bridge}]\right\} \left\{a_p\right\} = \overline{0} \end{aligned} \tag{10}$$

where $p = (m,n)$ and $q = (r,s)$.

In the following results we have increased step by step the number of unribbed plate's modes taken into account to stabilize the high-frequencies eigenfrequencies. This brings up to order p and q of 60 and 40 respectively.
Unlike matrices related to plate which are diagonal, those related to ribs and bridge are full and symmetric. So, superstructures introduce an important coupling of unribbed plate modes as we will see in the following sections.
The equation 10 becomes (harmonic form):

$$\left(\overline{\overline{K}} - \omega^2 \overline{\overline{M}}\right) \overline{a} = \overline{0} \tag{11}$$

where $\overline{\overline{K}}$ and $\overline{\overline{M}}$ are respectively generalized stiffness and mass matrices of the whole ribbed plate and $\overline{a}$ the vector of modal amplitudes a_{pq}.

4 Eigenvalue problem

The first study concerns the analysis of eigenmodes of the ribbed plate. The research of eigenvalues and eigenvectors of the $\overline{\overline{M}}^{-1}\overline{\overline{K}}$ matix leads us to a diagonal matrix of angular frequencies and to a matrix of eigenvectors whose terms are

the modal amplitudes weighting the unribbed plate's eigen modes to re-create ribbed plate's modes (see equation 7).

In this paper, we consider two cases of study:

- Case 1 : eleven ribs in the direction $\vec{y}$ pseudo-periodically spaced,
- Case 2 : the same ribs in the direction $\vec{y}$ and a bridge in the direction $\vec{x}$ (see figure 2).

Dimensions of the board and superstructures are taken from [6] (cheap upright piano's soundboard). We note that ribs' dimensions become less and less important when we go towards high keys (from right to left in the figure 2).
For this study the frequency range of interest is [0;5000] Hz. Let's consider the number of modes necessary to build a ribbed plate's mode. Figure 3 presents the evolution of this number in function of frequency. For that, we add the highest a_{pq} to approach more than 99% the real response.

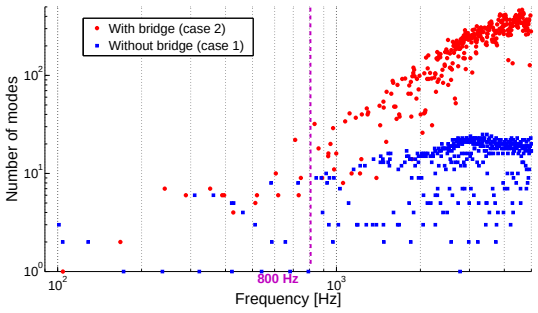

Figure 3: Evolution of the number of unribbed plate's modes taking part in the linear combination of ribbed plate's modes as a function of frequency.

Works of [5, 6, 7] show through statistical indicators (modal density) that a ribbed plate, and more particularly the piano soundboard, is similar to a homogeneous unribbed structure at frequencies lower of 800/1000Hz. Those modes appear at the abscissa of figure 3. We note that the number of homogeneous modes is higher in case 1 (ribbed in one direction) than case 2 (case 1 with a bridge). Beyond this frequency, the number of modes taken into account in the linear combination grows greatly and peaks to 25 for case 1 and 467 for case 2. So, the bridge brings a very important coupling and modal shapes are particularly complex. [6, 7] show also that localizations of vibrations appear when wavelength in the direction parallel to fibers is around inter-rib spaces. Our calculations show that majority of localizations takes place in the conditions described by the aforementioned authors. Nevertheless, it seems that many low frequencies modes are a linear combination of unribbed plate's modes, presenting moreover some localizations, and cannot be considered as homogeneous plate's modes (see figures 4 and 5).

In case 1 (ribbed in one direction), we see that differences of ribs' dimensions (heights and widths) create an asymmetry. From third mode to 800/1000Hz, the structure becomes homogeneous with a few localizations as for example the 6th mode at the frequency of 310 Hz (see figure 4).

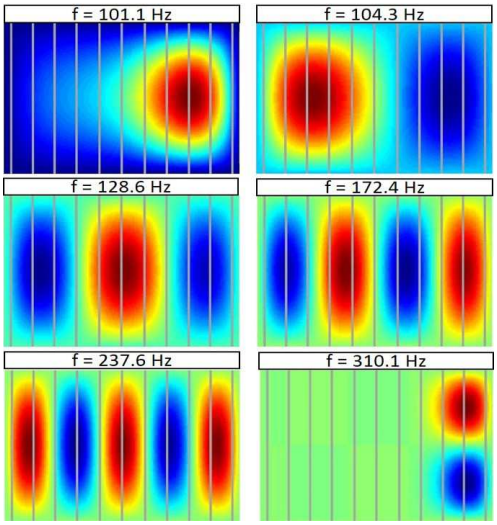

Figure 4: 1st to 6th modes for case 1 (one direction ribbed plate).

In case 2 (case 1 with a bridge), the soundboard seems to be separated in two parts. We often find a vibrating area and a non-vibrating area in each side of the bridge (see figure 5). In those conditions, only the first mode "doesn't see" the superstructures and corresponds to an unribbed plate's mode even if the second is not too far. However, taking into account the separating effect previously cited, we find modes like those of an unribbed plate localized on reduced soundboard delimited by the bridge. The bridge seems to "spread " the heights of different ribs along the plate and to homogenize it in the direction $\vec{x}$ for the first modes. We also find localizations out of conditions described by [6, 7] but those phenomenon are even less common than in case 1.

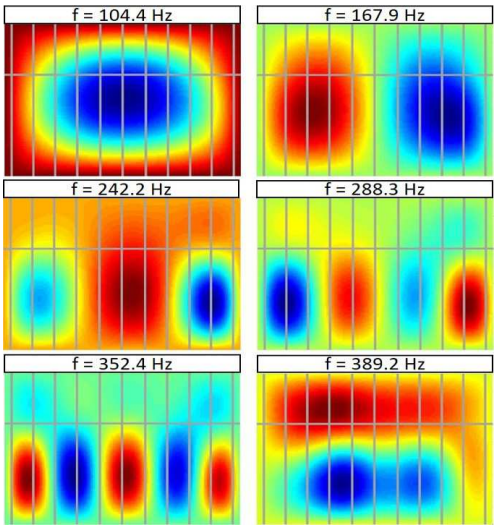

Figure 5: 1st to 6th modes for case 2 (ribbed plate with bridge).

In addition of the possibility of easy and quick parametric studies, the method that we develop allows to calculate quickly high-frequency modes. Figure 6 gives one of those modes which presents interesting vibrating phenomenon: oblique waves and localized wave's reflections between ribs.

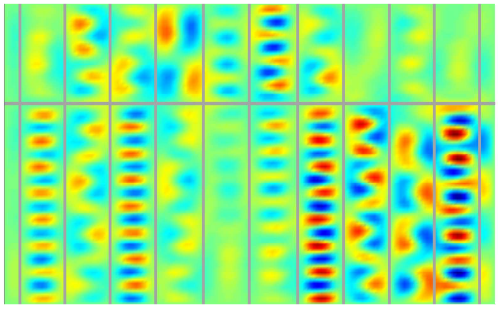

Figure 6: 288th mode for the case 2 (ribbed plate with bridge) of frequency of 4190 Hz presenting complex vibratory phenomenon.

5 Forced response

A second study concerns the response of the system for a particular excitation. We introduce an external effort $F(x_e, y_e, t) = F\delta(x - x_e)\delta(y - y_e)e^{j\omega_e t}$ which is harmonic, punctual (multiplication of diracs $\delta(x - x_e)\delta(y - y_e)$) and applied to the coordinates (x_e, y_e). We define the vector of generalized effort $\overline{F}_{gen}$ and those components are defined by the following relation :

$$F_{pq} = F\ \phi_{pq}(x_e, y_e) \tag{12}$$

We calculate then the vector of modal amplitudes for a particular excitation :

$$\overline{a} = \left(\overline{\overline{K}} - \omega_e^2 \overline{\overline{M}}\right)^{-1} \overline{F}_{gen} \tag{13}$$

Ege *et al.* show in [6] that the structural damping measured on the upright soundboard made of spruce in playing situation varies between 1% and 3%. We have chosen to apply a constant coefficient of 2% for all the frequencies by making complex the stiffness matrix $\overline{\overline{K}}$.

Mobility at the bridge is a classical measure in musical acoustic [4, 2, 3, 8] and [7] has shown that it is essentially dominated by the bridge in the mid- and high-frequency domain. It's defined by the ratio between the vibration velocity and the applied effort at the same application point. For a harmonic excitation, this mobility is calculated by :

$$Y(x_e, y_e, \omega_e) = \frac{|j\omega\ w(x_e, y_e, \omega_e|)}{F} \tag{14}$$

In order to validate the pertinence of the model, we compare our results with those of N. Giordano [4] and more particularly with an excitation on the bridge and another far from the bridge between two ribs. Because Giordano measured impedance ($|Z| = 1/|Y|$), our results will be presented in this form too. The geometry of the simulated plate is adapted to approach the best as possible the soundboard used during experiences by [4]. Unfortunately, we don't have all the information about this board: only are known dimensions of the soundboard, number and distance between ribs (measured on drawing of [4]). So, it's impossible to compare strictly our results to experimental data. In spite of those differences and unknowns, our results confirm those of Giordano as shows figure 7. Calculated impedances are in the same order of magnitude as those from literature and follow the tendencies of evolution measured. At the bridge, the mean value of impedance is comparable for the both plots. Far from the bridge, impedance calculated analytically is around three times smaller than those at the bridge; that corroborates the results of Giordano [4]. As indicated in [6, 7], we also find a sudden decrease of impedance when wavelengths in the perpendicular direction of the ribs are comparable to the inter-rib spaces.

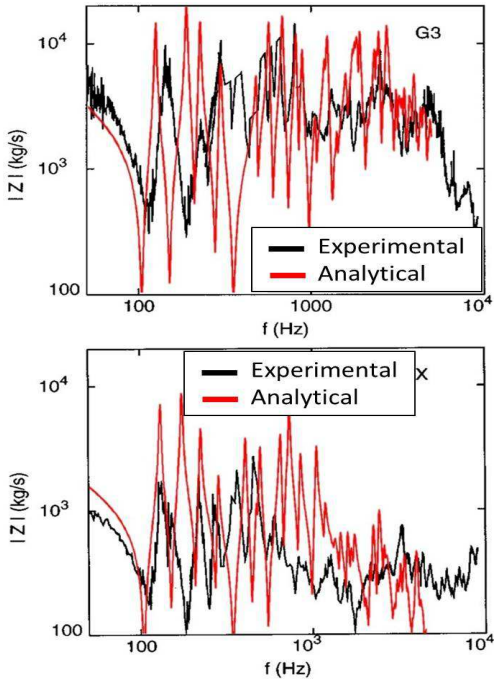

Figure 7: Comparison of impedances between the measurements of N. Giordano [4] and our analytical model. Top : at the bridge. ; Bottom : far from the bridge between two ribs.

6 Geometrical complexities of the soundboard

We want now to introduce geometrical complexities to evaluate their influences on the vibratory response of the piano soundboard. We are interested more particularly in the influence of cut-off corners: diagnoal rigid beams (see figure 1). In the model, we choose to add two lines of traction-springs in order to create a blocking along the two diagonals. A spring brings an extra strain energy and so an extra action. In that case, springs add a term to the Hamilton function. Let :

$$H_{tot} = H_{plate} + \sum_{i=1}^{N} H_{i^{th}\ ribs} + H_{bridge} + H_{springs} \tag{15}$$

Following the same approach that before, we calculate an extra rigidity matrix due to springs (which introduce new couplings).
We choose to put 6 springs per wavelength in order to block correctly the motion of the plate along each beam. For a frequency of 5000 Hz, it corresponds to a spring every 1 cm.

The influence of those geometrical complexities is presented in this paper in the case of a typical musical excitation. For simplicity reasons, the model chosen for this excitation corresponds to a *plucked* string rather than

struck. This model is taken from [11] and has been presented recently more in details in [13]. Let the following force at the bridge transmitted to the soundboard:

$$\widetilde{F}(\omega) = -T \sum_n \frac{2hL_c}{n\pi x_m(L_c - x_m)} cos(k_n L_c) sin(k_n x_m) \frac{1}{2} \delta(\omega - \omega_n) \tag{16}$$

where T, h, L_c, x_m and k_n are respectively the tension of the string, its initial amplitude, the length of vibrating string, the position where it's plucked and the wavenumber of the n^{th} harmonics of the strings.

Finally the velocity field of the soundboard is obtained by the same method as in the previous parts. We choose to present here the results in terms of quadratic velocity: $v_{note}(x,y) = \sqrt{\sum_n |j\omega_n\, w(x,y,\omega_n)|^2}$. The figure 8 shows the differences between a soundboard with and without cut-off corners for an excitation at the key A4 ($f_0 = 440$ Hz). We consider 10 harmonics in the force at the bridge (see equation 16). Note that the crosses on the following figures represent the application point of this force. We see that the vibration field is completely different in both cases. Indeed, because of their high rigidity, the diagonal beams keep the vibrations in the central area.

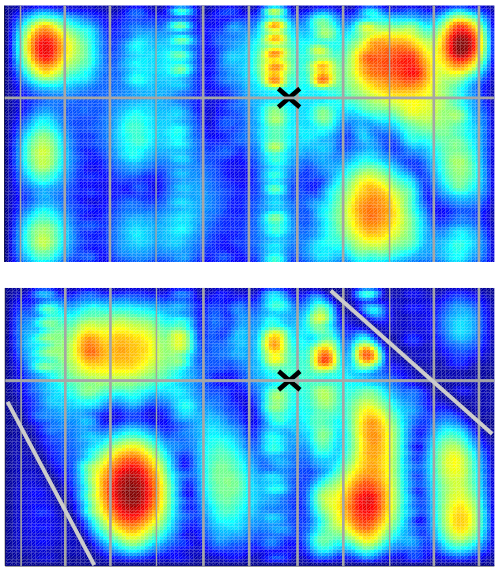

Figure 8: Vibratory response of the soundboard for an excitation of the key A4 ($f_0 = 440$ Hz).
Top : without cut-off corners. ; Bottom : with cut-off corners.

7 Conclusion

In this article, we have presented the basis of a new analytical modelling method for the vibrations of orthotropic ribbed plates with undescribed edges. Actually, we have limited here our study to the case of a rectangular plate with special orthotropy and small geometrical complexities. Results are encouraging and in good agreement with published results especially impedances at the bridge and far from the bridge but also eigenmodes and vibratory responses at typical frequencies. In order to validate the presented analytical numerical method, experimental and finite element modelling comparisons will be done.

Acknowledgments

This work was performed within the framework of the Labex CeLyA of Université de Lyon, operated by the French National Research Agency (ANR-10-LABX-0060/ ANR-11-IDEX-0007).

References

[1] I. Brémaud, Diversité des bois utilisés ou utilisables en facture d'instruments de musique, *Thèse de doctorat*, Université Montpellier II (2006).

[2] H. Suzuki, Acoustics of Pianos, *Applied Acoustics*, 30(2): 147-205 (1990).

[3] H. A. Conklin, Design and tone in the mechanoacoustic piano. Part II. Piano structure, *JASA*, 100(2): 695-708 (1996).

[4] N. Giordano, Mechanical impedance of a piano soundboard, *JASA*, 104(4): 2128-2133 (1998).

[5] J. Berthaut, M. N. Ichchou, & L. Jezequel, Piano soundboard : structural behavior, numerical and experimental study in the modal range, *Applied Acoustics*, 64(1): 1113-1136 (2003).

[6] K. Ege, X. Boutillon, & M. Rébillat, Vibroacoustics of the piano soundboard : (Non)linearity and modal properties in the low- and mid-frequency ranges, *JSV*, 332(5): 1288-1305 (2013).

[7] X. Boutillon & K. Ege, Vibroacoustics of the piano soundboard : Reduced models, mobility synthesis, and acoustical radiation regime, *JSV*, 332(18): 4261-4279 (2013).

[8] A. Chaigne, B. Cotté & R. Viggiano, Dynamical properties of piano soundboards, *JASA*, 133(4): 2456-2466 (2013).

[9] B. Laulagnet & J. L. Guyader, Sound radiation by finite cylindrical ring stiffened shells, *JSV*, 138(2): 173-191 (1990).

[10] B. Laulagnet & J. L. Guyader, Structural acoustic radiation prediction : expanding the vibratory response on a function basis, *Applied acoustics*, 43(3): 247-269 (1994).

[11] A. Chaigne & J. Kergomard, Acoustique des instruments de musique, *Belin*, (2008).

[12] X. Boutillon, Model for piano hammers: Experimental determination and digital simulation, *JASA*, 83(2): 746-754 (1988).

[13] B. Trévisan, K. Ege & B. Laulagnet, Développement d'une méthode analytique pour la prédiction des mécanismes vibro-acoustiques des plaques orthotropes raidies de formes quelconques : application à la table d'harmonie de piano, *Congrès Français d'Acoustique, CFA2014*, Poitiers, France (2014).